Terahertz waveform synthesis via optical rectification of shaped ultrafast laser pulses

J. Ahn, A. V. Efimov, R. D. Averitt, and A. J. Taylor

Los Alamos National Laboratory
Material Science and Technology Division
Los Alamos, New Mexico 87545, USA
jwahn@lanl.gov

Abstract: We demonstrate the use of optical pulse-shaping technique in conjunction with difference frequency generation in a non-linear optoelectronic crystal for generating synthesized waveforms at terahertz frequencies. Spectral phase modulations, programmed using Gerchberg-Saxton algorithm and prepared in a spatial light Fourier filter, produce tailored terahertz pulses, including chirped pulses, zero-area pulses, and trains of multiple pulses for tunable narrow-band terahertz radiation up to 2.0 THz.

OCIS codes: (320.5540) Pulse shaping; (190.7110) Ultrafast nonlinear optics

References and links

1. J. M. Chamberlain, and R. E. Miles, New Directions in Terahertz Technology (NATO Asi Series. Series E, Applied Sciences, Vol 334), (Boston, Kluwer Academic Publishers, 1997).
2. L. Xu, X.-C. Zhang, and D. H. Auston, "Terahertz beam generation by femtosecond optical pulses in eletro-optic materials," Appl. Phys. Lett. **61**, 1784-1786 (1992).
3. D. You, R. R. Jones, D. R. Dykaar, and P. H. Bucksbaum, "Generation of High-Power Half-Cycle 500 Femtosecond Electromagnetic Pulses," Opt. Lett. **18**, 290 (1993).
4. R. Huber, A. Brodschelm, F. Tauser, and A. Leitenstorfer, "Generation and field-resolved detection of femtosecond electromagnetic pulses tunable up to 41 THz," Appl. Phys. Lett. **76**, 3191-93 (2000).
5. C. Winnewisser, P. Uhd Jepson, M. Schall, V. Schyja, and H. Helm, "Electro-optic detection of THz radiation in $LiTaO_3$, $LiNbO_3$, and ZnTe," Appl. Phys. Lett. **70**, 3069 (1997).
6. Q. Chen, and X.-C. Zhang, "Polarization modulation in optoelectronic generation and detection of terahertz baams," Appl. Phys. Lett. **74**, 3435 (1999).
7. B. E. Cole, J. B. Willams, B. T. King, M. S. Sherwin, C. R. Stanley, "Coherent manipulation of semiconductor quantum bits with terahertz information," Nature **410**, 60 (2001).
8. R. Huber, F. Tauser, A. Brodschelm, M. Bichler, G. Abstreiter, and A. Leitenstorfer, "How many-particle interactions develop after ultrafast excitation of an electron-hole plasma," Nature **414**, 289 (2001).
9. D. M. Mittleman, M. Gupta, R. Neelamani, R. G. Baraniuk, J. V. Rudd, and M. Kock, "Recent Advances in terahertz imaging," Appl. Phys. B **68**, 1085-1094 (1999).
10. D. G. Tilley, and D. J. Yemc, "Wave domain processing of synthetic aperture radar signals," Johns Hopkins APL technical Digest **15**, 224-36 (1994).
11. J. Ahn, D. N. Hutchinson, C. Rangan, and P. H. Bucksbaum, "Quantum phase retrieval of a Rydberg wave packet using a half-cycle pulse," Phys. Rev. Lett. **86**, 1179-82 (2001).
12. Y. Nakamura, Yu. A. Pashkin, and J. S. Tsai, "Coherent control of macroscopic quantum states in a single-Cooper-pair box," Nature **398**, 786-788 (1999).
13. C. W. Siders, J. L. W. Siders, A. J. Taylor, S.-G. Park, and A. M. Weiner, "Efficient high-energy pulse-train generation using a 2^n-pulse Michelson interferometer," Appl. Opt. **37**, 5302 (1998).
14. A. M. Weiner, "Femtosecond pulse shaping using spatial light modulators," Rev. Sci. Instru. **71**, 1929 (2000);
15. R. Trebino, K. W. DeLong, D. N. Fittinghoff, J. N. Sweetser, M. A. Krumbugel, B. A. Richman, D. J. Kane, "Measuring ultrashort laser pulses in the time-frequency domain using frequency-resolved optical gating," Rev. Sci. Instru. **68**, 3277-95 (1997).
16. Y. Liu, S.-G. Park, and A. M. Weiner, "Terahertz waveform synthesis via optical pulse shaping," IEEE J. Quantum Electron. **2**, 709 (1996).

#2882 - $15.00 US
Received August 12, 2003; Revised September 17, 2003

17. S.-G. Park, A. M. Weiner, M. R. Melloch, C. W. SIder, J. L. Sider, and A. J. Taylor, "High-power narrow-band terahertz generation using large-aperture photoconductors," IEEE J. Quantum Electron. **35**, 1257-68 (1999).
18. G. Gallot and D. Grischkowsky, "Electro-optic detection of terahertz radiation," J. Opt. Soc. America B **16**, 1204-1212 (1999).
19. J.-P. Caumes, L. Videau, C. Rouyer, and E. Freysz, "Kerr-Like nonlinearity induced via terahertz generation and the elctro-optical effect in Zinc blend crystals", Phys. Rev. Lett. **89**, 047401 (2002).
20. A. Nahata, A. S. Weling, and T. F. Heinz, "A windeband coherent terhaertz spectroscopy system using optical rectification and electro-optic sampling," Apl. Phys. Lett. **69**, 2321 (1996).
21. R. W. Gerchberg and W. O. Saxton, "Phase determination from image and diffraction plane pictures in the electron microscope," Optik **35**, 237-246 (1972).
22. A. Rundquist, A. V. Efimov, and D. H. Reitze, "Pulse shaping with the Gerchberg-Saxton algorithm," J. Opt. Soc. Am. B **19**, 2468 (2002).
23. Y.-S. Lee, N. Amer, and W. C. Hurlbut, "Terahertz pulse shaping via optical rectification in poled lithium niobate," Appl. Phys. Lett. **82**, 170 (2003).
24. J. Y. Sohn, Y. H. Ahn, D. J. Park, E. Oh, and D. S. Kim, "Tunable terahertz generation using femtosecond pulse shaping," Appl. Phys. Lett. **81**, 13 (2002).
25. Our GaAs data is consistent with the spectral tunning data shown in Fig. 8 of Ref. [16].
26. C. W. Siders, J. L. W. Siders, A. J. Taylor, S.-G. Park, M. R. Mellock, and A. M. Weiner, "Generation and characterization of terahertz pulse trains from biased, large-aperture photoconductors," Opt. Letter **24**, 241 (1999).
27. Y.-S. Lee, T. Meade, T. B. Norris, and A. Galvanauskas, "Tunable narrow-band terahertz generation from periodically poled lithium niobate," Appl. Phys. Lett. **78**, 3583 (2001).

1. Introduction

The generation of coherent radiation across the electromagnetic spectrum has enabled the technologies that have a defining impact on life in the 21st century. However, a gap in technology exists in the terahertz (THz) frequency regime, between 100 GHz and 10 THz (wavelengths between 30 μm and 3 mm). Historically, it has been technically difficult to generate, manipulate, and detect radiation in this portion of the electromagnetic spectrum where electronics transitions to photonics. A desire to develop this wavelength regime is fueled by potentially important applications in remote sensing, communications, signal processing, materials characterization and control, biological and medical imaging, and non-destructive evaluation (NDE) [1].

Ultrafast laser technology has made significant contributions towards expanding photonics to the THz regime. The technique of terahertz time domain spectroscopy (THz-TDS) generates broadband, single cycle THz pulses of subpicosecond duration using resonant femtosecond(fs) optical excitation of biased semiconductor strip-lines or nonresonant optical rectification in electro-optic crystals [2, 3, 4]. The coherent detection of the THz electric field is similarly achieved using fs optical gating pulses. Since THz-TDS is a coherent free-space optically-gated technique it has distinct advantages in comparison to conventional far-infared (optical) detection techniques. The coherent nature of THz-TDS yields a much greater brightness in comparison to thermal sources and optical-gating discriminates against thermal background leading to, in some cases, a signal-to-noise ratio (S/N) approaching 10^6. Indeed, using an optoelectronic technique based on semiconductor strip-lines, a spatially and temporally coherent beam of THz radiation from 0.1 to 5 THz can be generated and detected with S/N $> 10^5$, while nonlinear optical methods based on optical rectification have generated 50 fs THz pulses with frequencies from 0.1 to $\sim$40 THz that are detected with S/N = 1000:1 [5, 6]. Further, THz-TDS measures the electric field (i. e., amplitude and phase) of the THz pulse with high linearity. Fourier transformation of the measured THz field, after propagation through a sample (and a suitable reference) allows for the direct experimental determination of both the real and imaginary parts of the dielectric response (or equivalently, conductivity) as a function of frequency obviating the need for delicate Kramers-Kronig analysis. The THz pulses are derived from a coherent optical source, enabling synchronized optical excitation useful both for time-resolved spectroscopic studies and two-color schemes for communications, remote sensing, imaging, and signal processing [7, 8, 9].

#2882 - $15.00 US Received August 12, 2003; Revised September 17, 2003

For many of the envisioned applications of THz technology, the ability to generate and manipulate the radiation in a variety of formats is required. For example, temporally shaped pulse trains will be needed for communications, signal processing and materials control, broadband pulses for remote sensing and materials characterization, and tunable narrow-band radiation for enhanced imaging. Specialized applications such as quasi-optical synthetic aperture radar (SAR) for surveillance purposes require a frequency-chirped waveform [10]. The need for such spectrally sculpted pulses in the THz regime is further motivated by the routine use of such pulses in both optical and radio frequency applications [11, 12]. For visible and near-infrared wavelengths, ultrafast optical pulse shaping [13, 14], combined with ultrafast, phase-sensitive optical diagnostics such as frequency-resolved optical gating (FROG) [15] are well-established techniques for generating and characterizing nearly arbitrarily shaped ultrafast optical waveforms. This technique involves linear filtering of spatially separated frequency components from the large bandwidth of an ultrashort optical pulse. A grating and lens are used to image the spectrum of an ultrashort pulse onto a spatially varying mask, which can amplitude modulate and/or phase shift different frequency components. A subsequent lens and grating are used to combine the spectrally filtered components, producing a shaped waveform in the time domain. Since a spatial light modulator (SLM) can be used as a programmable mask, the optical waveform generation can be computer controlled, using adaptive feedback if necessary.

A promising approach for versatile THz waveform synthesis is the combination of ultrafast pulse shaping with optoelectronic or nonlinear optical THz generation schemes. The generation of THz waveforms, including the demonstration of phase modulation within the THz waveform, time-division multiplexing, narrow band amplitude modulation and the tunable narrow band THz generation, have been obtained using shaped ultrafast optical pulses to drive photoconductive emitters [16, 17]. In this paper, we explore a similar approach for the generation of arbitrary THz waveforms using optical rectification of shaped optical pulses in nonlinear crystals. THz generation via optical rectification has potential advantages in terms of increased bandwidth and versatility when compared to photoconductive schemes. Here, we present our results on the generation of THz pulse trains with repetition rates of up to 2.0 THz, as well as the generation of special THz pulses including chirped pulses and area pulses.

2. Model calculation

THz pulses generated from an optoelectronic crystal such as ZnTe may be calculated using the nonlinear Maxwell equation [18] expressed in the spatio-frequency domain for the difference frequency mixing of the optical pump laser pulse. The local THz field is proportional to the second-order time derivative of the second-order nonlinear polarization induced via optical rectification. If we assume that the pump laser pulse propagates in the z-direction and has a Gaussian temporal profile with a pulse width of τ_G, the simplified equation may be written as

$$\frac{\partial^2}{\partial z^2}E^{\mathrm{THz}}(z,\omega) \quad + \quad \varepsilon(\omega)\frac{\omega^2}{c^2}E^{\mathrm{THz}}(z,\omega) = -\frac{4\pi\omega^2}{c^2}P^{(2)}(z,\omega), \tag{1}$$

where the polarization $P^{(2)}(z,\omega)$ is the product of the second order nonlinear index $\chi^{(2)}(\omega)$ and the Fourier transform of the intensity of the pump laser pulse $\widetilde{I}(\omega) = \widetilde{I_o}\exp(-(\tau_G\omega)^2/2)$, or

$$P^{(2)}(z,\omega) = \chi^{(2)}(\omega)\widetilde{I}(\omega)\exp(i\omega z/v_g), \tag{2}$$

where v_g is the group velocity of the optical pulse. The solution for this nonlinear Maxwell equation, similar to Eq. (2) in Ref. [19], is obtained at each point of the non-linear crystal as

$$E^{\mathrm{THz}}(z,\omega) \propto \omega^2\chi^{(2)}(\omega)\widetilde{I}(\omega)z\mathrm{sinc}(\frac{\triangle k^{\mathrm{THz}}z}{2}), \tag{3}$$

#2882 - $15.00 US Received August 12, 2003; Revised September 17, 2003

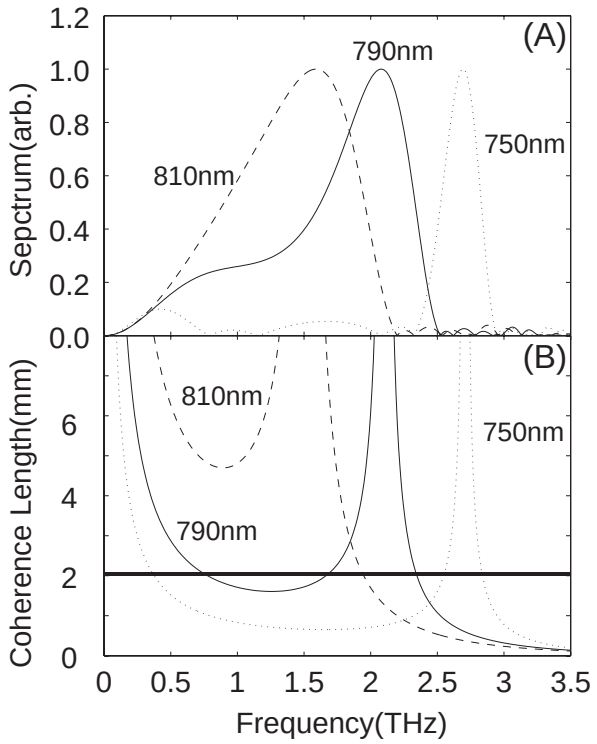

Fig. 1. Terahertz spectrum and coherence length in ZnTe. Terahertz spectra(upper figure) for three different pump laser wavelengths (810, 790, and 750 nm) are shown compared with the coherence lengths (lower figure) defined as $l_c = \pi/\triangle k$. The thickness of the ZnTe crystal, indicated under the thick line, is chosen to separate the coherent bands in the spectrum for 790 nm and 750 nm.

where $\triangle k^{\mathrm{THz}} = k - \omega/v_g$ is the momentum mismatch between the THz pulse and the optical pump laser pulse, which may also be written as $\triangle k^{\mathrm{THz}} = \pi/l_c(\omega)$, where the coherence length $l_c(\omega;\lambda)$[20] is

$$l_c(\omega;\lambda) = \frac{c}{2f}\left|n_o(\lambda) - \lambda dn_o(\lambda)/d\lambda - n_t(\omega)\right|. \tag{4}$$

where n_o and n_t are the refractive indexes at optical and THz frequencies respectively.

The spectrum for the generated THz pulse propagating through a ZnTe is obtained by integrating Eq. (3) over the crystal thickness z_o. Once the THz pulse travels a distance equivalent to the coherence length of this non-linear frequency mixing process, the spectral shape of the THz pulse is greatly altered. The calculated results are shown in Fig. 1(a), where the spectral shapes are primarily governed by the coherence length of the thick crystal. As the pump laser wavelength is tuned below 790 nm, most of the low frequency parts of THz spectra becomes phase-mismatched as shown in Fig. 1(b), and the obtained THz spectra are quite narrow. For comparison, the experimentally measured spectra and pulse shapes are shown in Fig. 2. Here the thickness of the ZnTe crystal is chosen to separate the coherent band of the THz spectrum into two, one at near zero frequency and the other at higher frequencies. This results in two distinct spectra humps as shown in Figs. 2(b) and (c). The obtained spectrum for the generated THz pulse is strongly dependent on the pump laser wavelength and the temporal shapes vary from a single-cycle pulse with pulse duration of 250 fs to an oscillating pulse stretched out to

#2882 - $15.00 US
Received August 12, 2003; Revised September 17, 2003

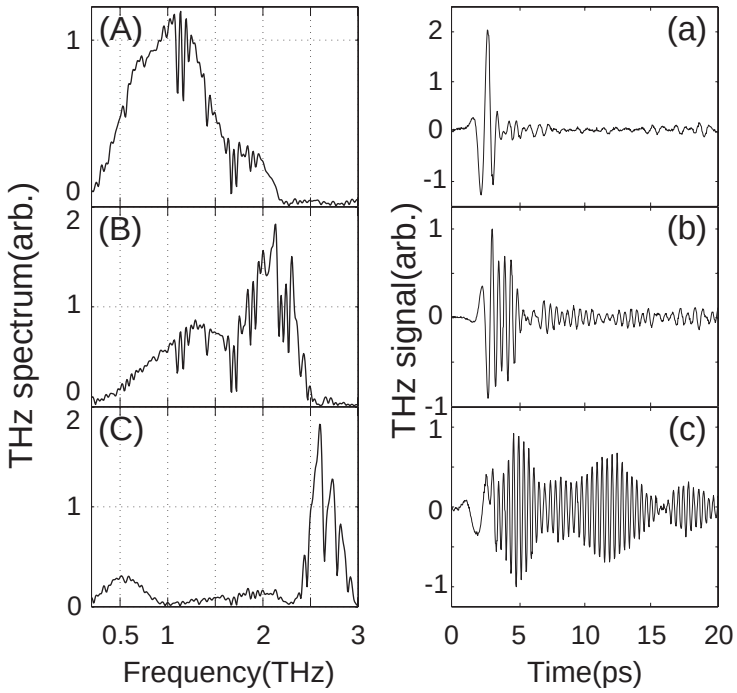

Fig. 2. Measured terahertz spectra(left panel) and their far-field waveforms(right panel) at three different excitation wavelengths : (a) λ=810 nm; (b) λ=790 nm; (c) λ=750 nm.

over 50 ps in time as in Fig. 2(c).

3. Experiments

A schematic diagram of the experimental setup is shown in Fig. 3. The Ti:sapphire oscillator produces $\sim$150 fs pulses at a repetition rate of 80 MHz with a wavelength centered at 810 nm, chosen to generate the shortest THz waveform from a gaussian-shaped optical pulse for best temporal resolution, as described above. The output of the oscillator is split into two beams, with one beam input into the pulse shaper and one used to gate the ZnTe THz detector. The pulse shaping apparatus [14] consists of a pair of 1800 lines/mm gratings placed at the focal planes of a unit magnification confocal lens pair (15 cm focal length). Optical pulse shaping is accomplished using a programmable liquid crystal modulator (LCM) manufactured by Cambridge Research Inc. The 128-element LCM induces individual phase retardation on the pulse spectrum. The cross-correlation, measured via second harmonic generation, between the shaped optical pulse and an unshaped reference pulse reveals the intensity profile of this shaped optical pulse. The shaped pulse is focused to a $\sim$100 μm diameter spot on a 2 mm-thick (110) ZnTe crystal. The generated THz radiation is collimated using an off-axis parabolic mirror and propagates for 20 cm before it is refocused using an identical parabolic mirror. The temporally varying amplitude and phase of this tailored THz pulse train are measured via electro-optic sampling in a second, identical, ZnTe crystal using the unshaped optical pulse split off from the output of the Ti:sapphire oscillator before the pulse shaper. The temporal shape of the THz field is mapped out by varying the delay between the shaped pulse and the gate pulse.

#2882 - $15.00 US
Received August 12, 2003; Revised September 17, 2003

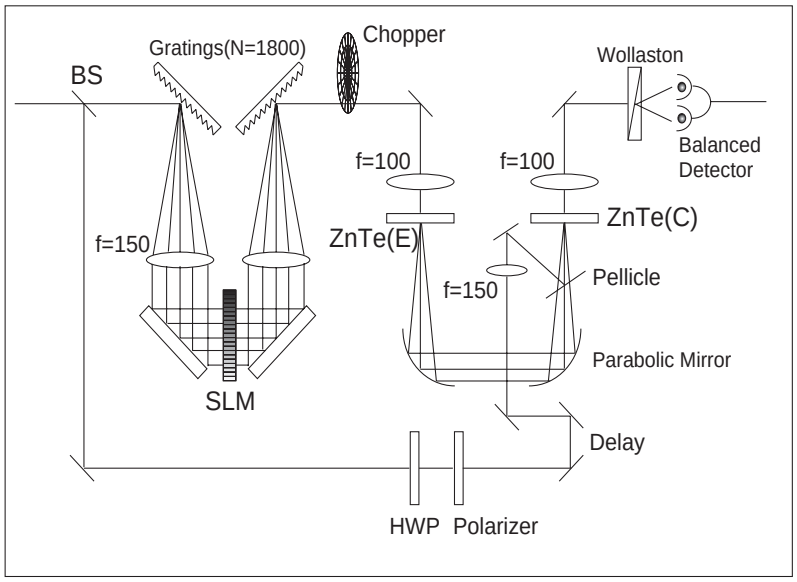

Fig. 3. Schematic diagram of experimental arrangement. Pump laser pulses enter the apparatus from the left and are spectrally dispersed in an optical pulse shaper which has a computer-controlled array of optical masks before combined without spatial dispersion. The programmed optical pulses now generate the shaped terahertz pulses. The shape of the terahertz pulses are recorded as the phase modulation in the electro-optic ellipsometer, and analyzed via a fast lock-in detection.

4. Terahertz waveform synthesis

The design of the THz waveforms was performed via spectral shaping of the pump laser pulse in a phase-only pulse shaper. The desired optical intensity targets typically consisted of trains of pulses with variable pulse widths and pulse separations in the time domain. Since phase-only shaping is not capable of absolutely arbitrary shaping, an approximate method was used implemented using the Gerberg-Saxton (GS) algorithm [21, 22]. Based on the input pulse spectrum and the intensity target in the time domain, this algorithm computes the desired spectral phase profile which yields the best approximation of the target waveform. Although other algorithms, such as the genetic algorithm, can be used to compute the phase masks, the GS was shown to yield good results with near-real time performance and it is simpler to implement and operate. The GS algorithm finds a particular spectral phase function which, when combined with an input intensity spectrum, will yield a shaped temporal intensity profile as close to the target as possible. On each iteration the GS algorithm makes use of two constraints (invariants) of the problem in two conjugate domains: (i) the input pulse spectrum, unaffected by phase filtering, and (ii) the temporal intensity target. Initially the pulse spectrum is Fourier-transformed into the time domain, assuming a random phase, where the amplitude is replaced with the target while the phase is retained. Fourier transform back to frequency domain is then performed where the spectral amplitude is replaced with the input pulse spectrum and the phase is again retained without change. On the last iteration this phase constitutes the desired phase mask. Typically, the algorithm converges in a few iterations, although several hundred iterations are sometimes required for complex target waveforms.

The spectral content of THz pulse trains can be easily shaped by weaving multiple simple waveforms with programmed phase delays [23]. We have demonstrated two types of spectrally

#2882 - $15.00 US Received August 12, 2003; Revised September 17, 2003

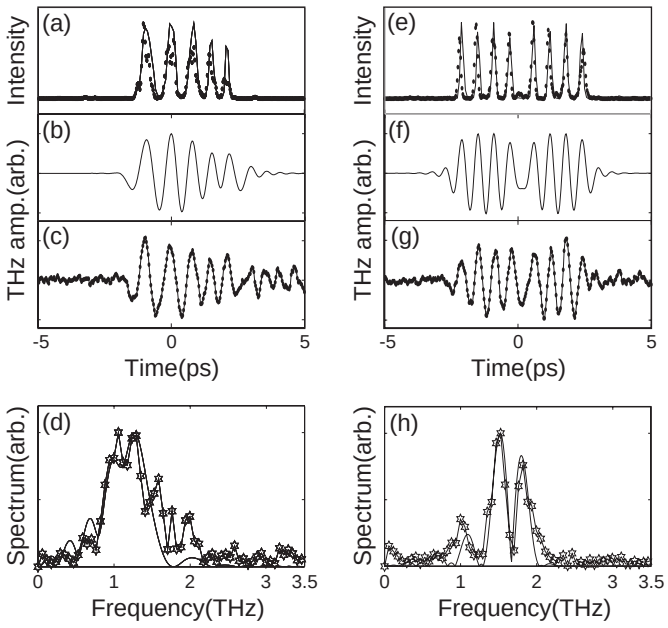

Fig. 4. Demonstration of the chirped terahertz pulse and the zero-area terahertz pulse. The optical pulse trains programmed via Gerchberg-Saxton algorithm for chirped pulse (a) and zero-area pulse (e) (dots - experimental cross-correlations, lines - numerical targets), terahertz waveforms designed and measured for the designed chirped pulse (b,c) and the zero-area pulse (f,g), the calculated (line) and measured (hexagon) spectra of chirped pulse (d) and zero-area pulse (h).

shaped THz waveforms in THz frequency region. The chirped-pulse shown in the left panel of Fig. 4 has temporally delayed spectral components. The chirping ratio was kept as $dw/dt \approx 0.5$(THz/ps). The full bandwidth of a single impulsive THz pulse was kept in a train of five THz pulses in such a way that the temporal spacings of the pairs of adjacent THz pulses were decremented. The widths of the pulses are also designed to be decremental in order to keep the individual waveforms spectrally in phase with each other. The Gaussian pulse widths and the temporal locations of the individual optical pulses are $\tau_k = 125(1+0.50(k+3))$ fs, and $t_o^k = 700k(1+0.08(k+3))$ fs, where $k = -3,-2,\cdots,1$. The temporal shape of the optical pulse train is shown in Fig. 4(a), where the dots represent the experimental cross-correlations and the line is the numerical calculation. The shape of the optical pulse train is calculated using the GS algorithm as explained above. The THz waveforms obtained from the calculation and the experiment are shown in Fig. 4(a) and Figs. 4(b) and (c), respectively. The target waveforms of the temporal and spectral shapes in Figs. 4(b) and (c) are calculated using Eq. (3). The experimental THz spectrum in (d) of the same figure agrees well with the spectrum of the designed THz pulse.

These results show that chirped-pulses provide a way to maintain the full spectral bandwidth of a single THz pulse even in a train of THz pulses, by temporally delaying the spectral components in time. On the other end, a zero-area pulse provides a way to reduce the spectral bandwidth. In a zero-area pulse, one half of the pulses in a THz pulse train maintain the opposite phase with respect to the other half of the pulses in the same pulse train. Then, the two temporally delayed parts in a single pulse train have exactly the opposite spectral phase with respect to each other. This results in destructive interference between them in the spectral domain.

#2882 - $15.00 US
Received August 12, 2003; Revised September 17, 2003

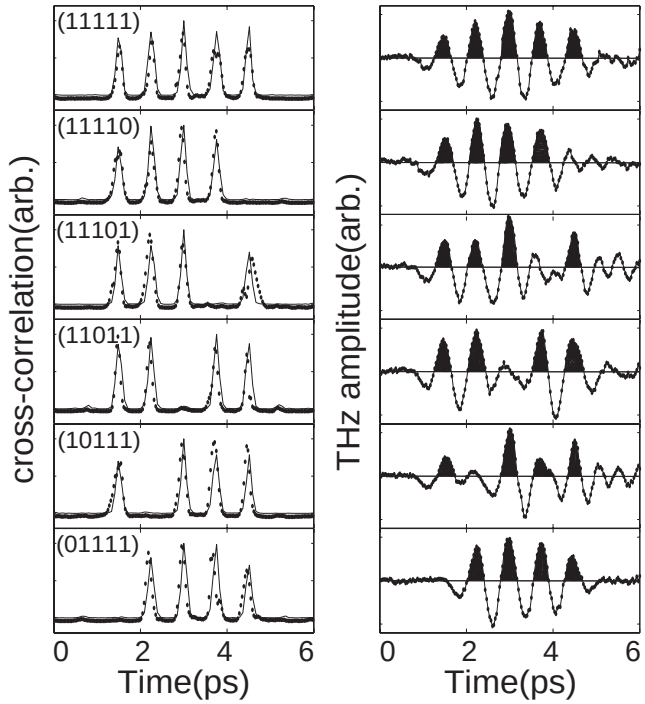

Fig. 5. Digital pulse demonstration. The terahertz binary signal is represented by the negative amplitudes of the electric field pulse. From the top of the figure, the binary numbers (11111), (01111), (10111), (11011),(11101), and (11110) are encoded.

The feature shows a very sharp spectral peak with a dip in the middle of the spectrum. In order to design this zero-area pulse, we have used eight optical pulses with the same Gaussian pulse width of $\tau_k = 250$ fs but with different temporal delays $t_o^k = 750(k - 0.5H(0.5-k))$ fs, where $H(x)$ is the Heaviside step function ($H(x) = 1$ for $x > 0$ and 0 for $x < 0$) and $k = -3, -2, \cdots, 4$. The temporal shape of the optical pulses is shown in Fig. 4(e). The temporal and spectral profiles of the designed THz waveform are shown in Fig. 4(f), (g), and (h). The π-phase shift at time zero is observable in both THz waveforms in (f) and (g) in the same figure. The spectral shapes in Fig. 4(h) show the described spectral feature as expected.

Fast electronic switching can be achieved using THz waveform synthesis in the temporal domain. The positive (or negative) amplitude of the electric field of a THz pulse train can be mapped one-to-one to a binary zero-one sequence. As shown in the left panel of Fig. 5, the temporally separated optical laser pulses are easily programmed by the GS algorithm, and the fast response of the nonlinear opto-electronic ZnTe converts the optical intensity, which is temporally varying, to THz frequencies. The positive amplitudes (marked in black) of the THz pulses shown in the right panel of the same figure agree well with the encoded bit information of the optical pulse trains. In this experiment, we have used the amplitude of the THz pulses to encode bit information. From top to the bottom, the THz pulses carry (11111), (01111), (10111), etc. We notice that the designed THz sequence appears somewhat distorted due to the temporal ringing of the individual THz pulses, making it difficult to decode information from their temporal shapes. In order to minimize the contribution from the temporal ringing of the previous THz single pulse to the following THz pulse, we have used 750 fs separation between THz pulses. This separation results in each successively generated THz pulse ringing to have

#2882 - $15.00 US
Received August 12, 2003; Revised September 17, 2003

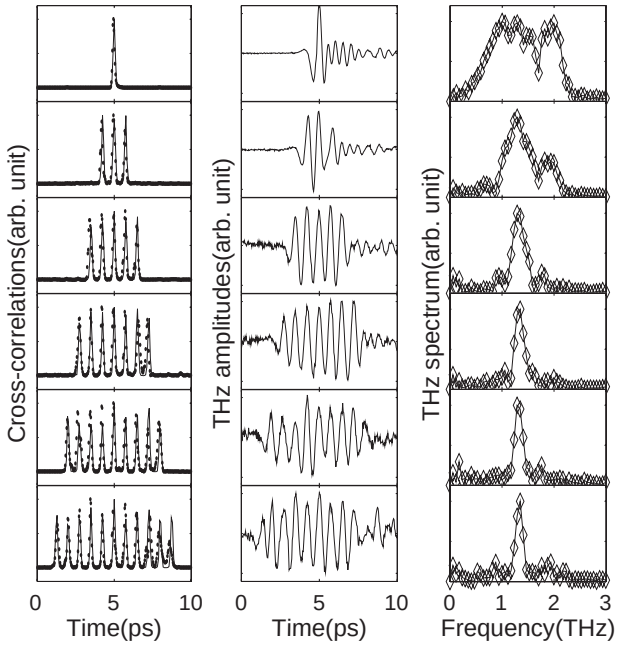

Fig. 6. Temporal and spectral shapes of designed terahertz pulses for demonstrating the narrowing of the spectral width. From top to bottom, 1, 3, 5, 7, 9, and 11 cycle pulses are programmed. The intensity of the optical pulses, the temporal shapes, and the spectra of the terahertz pulses are shown in the left, the middle, and the right panels, respectively. The oscillatory pulse trains are prepared by weaving multiple impulsive terahertz pulses.

the opposite phase with respect to the previous pulse.

The number of pulses in the train of optical pump pulses and their spacing can be used to narrow the resulting THz spectrum and to tune its central frequency [24]. In Fig. 6, we have programmed six different phase masks in order to generate incremental numbers of pulses with equal amplitudes. As shown in the central panel, the number of THz oscillations increases from 1 (top) to 11 (bottom). The increasing number of THz oscillations narrows the spectral bandwidth from 1.5 THz down to 0.2 THz in the right panel. This narrow-band THz pulse was prepared by a train of single THz pulses individually generated by an optical pulse train shown in the left panel. In Fig. 7, we have used the spacing of the pulses in a THz pulse train to tune the THz frequency. The optical pulse train, which has many nearly identical optical pulses with equal spacings between the neighboring pulses, was programmed in a temporal window of 10 ps. The width of the programmable temporal window was limited by the spatial separation of the spectral filters and the spectral resolution of the pulse shaper was $\sim$100 GHz. From top to bottom, the frequency of the THz source is tuned to 2.0, 1.8, 1.4, 1.2, 1.0, 0.8, and 0.5 THz. The highest frequency obtained in our experimental setup with ZnTe was 2.0 THz. THz pulses in a programmed THz pulse train for frequencies above 2.0 THz start to overlap with each other, contributing to a slow DC-drift in the temporal shape or a low frequency hump in the spectral profile. For comparison, in the right panel of Fig. 8, we show data using a biased GaAs crystal with 500 μm thickness with (100) orientation. The highest THz frequency achieved with this GaAs setup was 1.0 THz, if we apply the same restriction of no DC-drift in the temporal shape. In Fig. 8, the obtained THz spectra at 1.0, 0.8, and 0.5 THz (three top rows) are compared with the 1.3 THz (the bottom row) spectra. The temporal shape of the THz pulse giving the 1.3 THz

#2882 - $15.00 US
Received August 12, 2003; Revised September 17, 2003

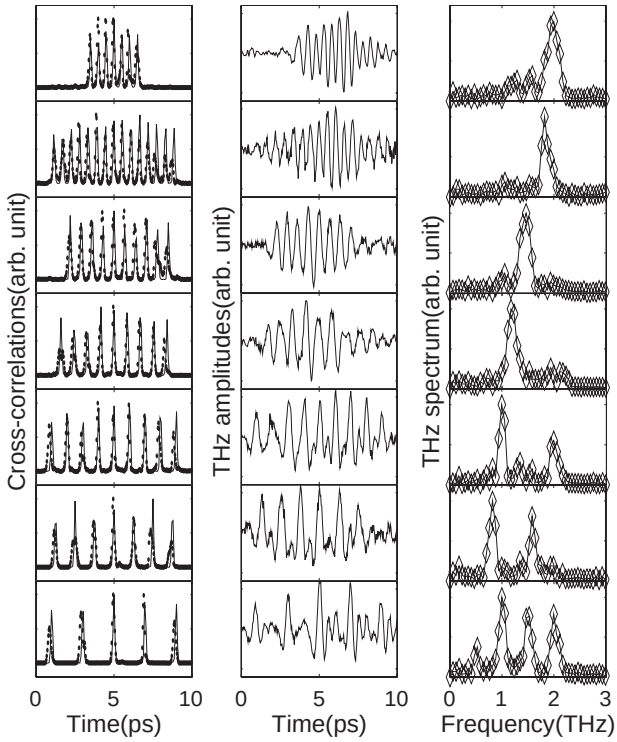

Fig. 7. Tuning of the terahertz spectrum from 0.5 THz to 2.0 THz generated from a thick ZnTe material with programmed optical pulse trains. The temporal intensity (the left column), terahertz waveforms(the middle column), and the spectral shapes (the right column) are shown. The temporal window of 10 ps (except the top experiment for 2.0 THz) was used to program a narrow-band tunable terahertz source. The frequency changes from 0.5 THz (bottom) to 2.0 THz(top).

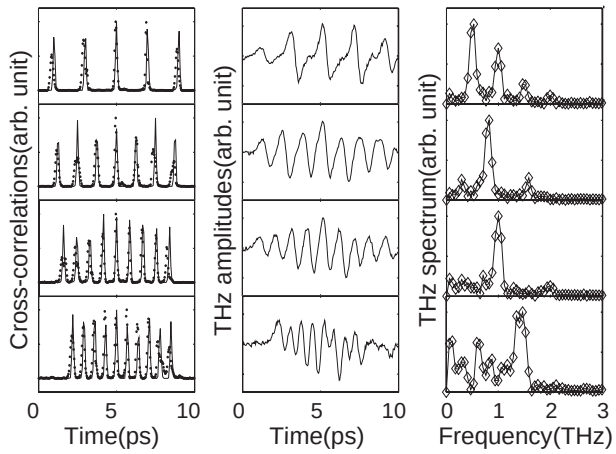

Fig. 8. Terahertz waveforms tuning the THz spectrum from 0.5 THz to 1.0 THz generated from a biased GaAs material with programmed optical pulse trains. The frequency changes from 0.5 THz (top) to 1.3 THz (bottom)

#2882 - $15.00 US
Received August 12, 2003; Revised September 17, 2003

spectra show severe distortions due to the temporal overlap between adjacent single THz pulses. Also the spectral shape has a significant near DC component [25]. In this GaAs experiment, the pump laser fluence was below the THz saturation regime in which the generation of THz pulse train would be greatly hindered by carrier depletion [26].

5. Discussion

Since optical rectification is a second-order nonlinear optical process, the peak intensity of the shaped optical pulses is critical to efficient THz pulse generation. For more complex optical pulses the low optical pulse intensity can limit the complexity of THz pulse shapes that can be programmed. For example, in order to produce a narrow-band tunable THz source, multiple optical laser pulses extending over several ps are required. In the implementation of optical pulse shaping in Fourier domain as achieved in this paper, the temporal width of the shaped optical laser pulse is inversely proportional to the spectral resolution of the Fourier filter. In our experiments we have used a temporal window of 10 ps to produce narrow-band THz pulses with a spectral width of $\sim$0.2 THz, and a $\sim$5 ps temporal window for more complex THz shapes. These parameters were optimally chosen considering the laser bandwidth, the Fourier filter resolution, and the pulse energy. Note that the complex waveforms described here were produced with an oscillator only. An alternative approach is THz pulse shaping in pre-engineered crystal domain structures [23, 27]. In this time-domain THz pulse shaping technique, Lee and co-workers have demonstrated THz pulses as narrow as 0.02 THz, tunable up to 2.5 THz but, in this method, generating different THz pulses requires physically different filters. Computer-controllable version of temporal filters of this kind have yet to be developed.

6. Conclusions

In conclusion, we have used non-linear difference frequency mixing of an optical coherent light source to produce designed THz waveforms. The THz waveforms are designed indirectly through temporal shaping of the optical pump laser pulses. In order to design and shape the optical laser pulses, we have used computer-generated phase masks calculated using the Gerchberg-Saxton algorithm and implemented in a high precision spatial light modulator with 128 parallel phase masks. We have demonstrated tailoring spectral shapes of THz waveforms including chirped THz pulses and zero-area THz pulses, by temporally weaving THz single pulses with programmed phase delays. We have demonstrated a stream of THz pulses which carries bit information with a rate of $1/500$ fs. This bit information was encoded using the polarity of the electromagnetic field. The method of shaping THz waveforms through difference frequency mixing in a non-linear crystal shown in this paper is not limited by the time scales of the real carrier dynamics which often hinders many fast optoelectronic applications of GaAs photoconductors. This THz pulse shaping technique, in conjunction with ultrashort THz pulses as short as 50 fs currently achievable would enable electronic switching and multiplexing as fast as 20 THz.

Acknowledgments

The authors acknowledge J. Y. Sohn and J. C. Madison for their help. This work was supported by the Laboratory-Directed Research and Development Programs at Los Alamos National Laboratory.

#2882 - $15.00 US Received August 12, 2003; Revised September 17, 2003